Kondo Correlations and Majorana Bound States in a Metal to Quantum-Dot to Topological-Superconductor Junction

A. Golub, I. Kuzmenko, and Y. Avishai
Department of Physics, Ben-Gurion University, Beer Sheva 84105, Israel
(Received 13 May 2011; published 17 October 2011)

Electron transport through a normal-metal–quantum-dot–topological-superconductor junction is studied and reveals interlacing physics of Kondo correlations with two Majorana fermions bound states residing on the opposite ends of the topological superconductor. When the strength of the Majorana fermion coupling exceeds the temperature T, this combination of Kondo-Majorana fermion physics might be amenable for an experimental test: The usual peak of the temperature dependent zero bias conductance $\sigma(V = 0, T)$ splits and the conductance has a *dip* at $T = 0$. The heights of the conductance side peaks decrease with magnetic field.

DOI: 10.1103/PhysRevLett.107.176802 PACS numbers: 73.43.−f, 73.23.−b, 74.45.+c

Introduction.—Recent theoretical investigations of topological materials reveal that topological superconductors can host Majorana fermions (MF) [1–8]. Specifically, Majorana bound states (MBS) reside at the opposite ends of a 1D topological superconductor (TS). Interest in the physics of Majorana quasiparticles is due to their non-Abelian statistics [9]. Hopefully, MBS can be realized on a 1D edge of a 2D quantum spin Hall insulator with superconducting gap induced by proximity effect [10,11], or at the ends of a 1D semiconducting wire with spin-orbit coupling, in proximity with an s-wave superconductor [3,5]. In both cases a 1D TS is formed. Two MF can form a neutral Dirac fermion, but its detection requires nonlocal measurements. The physics of MBS might also be probed in a tunneling process [12–14], namely, a local measurement sensitive to interference between various MBS.

Present work.—Motivated by the above findings, we consider as in Fig. 1 electron tunneling through a normal-metal–quantum-dot–topological-superconductor (NM-QD-TS) junction composed of NM lead, QD, and 1D TS. [Direct NM-TS tunneling conductance (without a dot) in 1D TS was considered in [15].] For the TS we analyze a particularly simple system: a 1D semiconducting wire with strong Rashba spin-orbit coupling, brought into proximity with an s-wave superconductor [16,17]. To drive the wire into a topological state one may subject it to a perpendicular magnetic field $\mathbf{B}$ [3] (that might also act on the dot). In the absence of interaction, the topological transition takes place at rather strong field ($B > \Delta$). However, recent analyses [16(b)] that incorporate strong repulsive interaction extend the parameter range over which the TS phase exists, achieving a TS phase even at zero magnetic field. Since the TS hosts two MBS on its ends [16,18], then, within a reasonable approximation, the tunneling problem is reduced to that of transport in a NM-QD-MBS junction. Our interest is focused on the interrelation between the Kondo physics prevailing in the quantum dot and the MBS physics prevailing on the TS. The analysis is naturally divided into the weak ($T \gg T_K$) and strong ($T < T_K$) coupling regimes, where T_K is the Kondo temperature. The effect of a magnetic field acting on the dot (through a Zeeman term) is also analyzed.

The central point of our analysis is that the Kondo effect in tunneling through QD is a useful tool for identifying MBS at the ends of TS due to the strong temperature dependence of the zero bias conductance, which, in itself, is sensitive to the unique (length dependent) interaction of the two MF. In other words, the Kondo effect determines the temperature dependence of the conductance for different MF couplings, a property that is exposed by plotting the zero bias conductance as function of temperature (see Fig. 5 below).

Junction Hamiltonian.—The system's Hamiltonian $H = H_0 + H_A + H_M$ includes the following components (see Fig. 1). (1) H_0 for the normal-metal lead, held at bias voltage V. (2) The Anderson Hamiltonian $H_A = H_{\text{TS-NM}} + H_{\text{QD}}$ for QD hybridized with the normal-metal lead and the TS. (3) The Majorana term H_M describes coupling of strength ν between two MF 1, 2 on the left and right ends of the TS. Employing Nambu formalism in four-dimensional (spin) ⊗ (electron-hole) space, where fermion operators (c for the lead and d for the dot) are written as $c = (c_\uparrow, c_\downarrow, c_\downarrow^\dagger, -c_\uparrow^\dagger)^T$, we have

$$\begin{aligned} H_0 &= \frac{1}{2}\sum_{\mathbf{k}} \varepsilon_{\mathbf{k}} c_{\mathbf{k}}^\dagger \tau_z c_{\mathbf{k}}, \\ H_{\text{TS-NM}} &= \frac{1}{2}[d^\dagger \tau_z \hat{V} \gamma_1 + t d^\dagger \tau_z c(0)] + \text{H.c.}, \\ H_d &= \frac{1}{2}[\varepsilon d^\dagger \tau_z d + U n_{d\uparrow} n_{d\downarrow}], \\ H_M &= \frac{i}{2}\sum_{i,j=1}^{2} \hat{\nu}_{ij} \gamma_i \gamma_j. \end{aligned} \tag{1}$$

Here γ_i ($i = 1, 2$) are MF operators satisfying $\gamma_i = \gamma_i^\dagger$, $\gamma_i^2 = 1$ coupled by an antisymmetric $2 \otimes 2$ matrix

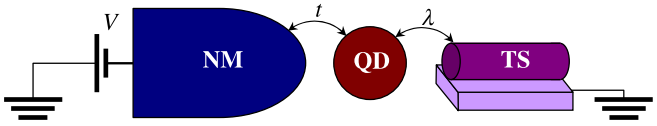

FIG. 1 (color online). NM-QD-TS junction. An applied magnetic field can induce MBS at the ends of the TS wire. The QD can be gated to adjust the level position in the dot.

$$\hat{\nu} = \nu \begin{pmatrix} 0 & 1 \\ -1 & 0 \end{pmatrix}.$$

$c(0)$ is the normal-metal lead electron operator at the QD position $x = 0$. The coupling between the quantum dot and Majorana states is proportional to the Majorana wave function at $x = 0$; hence, it strongly depends on the Rashba spin-orbit coupling. The coupling is presented by a vector which has a form depending on the direction of B. In our case [3] this vector is $\hat{V}_i = (\lambda_\uparrow, \lambda_\downarrow, \lambda_\downarrow^*, -\lambda_\uparrow^*)^T$. The Pauli τ matrices act on $(c_\sigma; d_\sigma; \lambda_\sigma)$ and $(c_\sigma^\dagger; d_\sigma^\dagger; \lambda_\sigma^*)$ blocks. Below we put $\lambda_\uparrow = \lambda$, $\lambda_\downarrow = -i\lambda$ [18]. Applying Schrieffer-Wolff transformation on H_A the Kondo Hamiltonian $H_K = H_{LK} + H_{KM} + BS_z$ with Zeeman energy is derived. In Nambu space we have

$$\begin{aligned} H_{LK} &= \frac{J_L}{2} c^\dagger(0) Q \tau_z c(0), \\ H_{KM} &= \frac{t}{|\varepsilon|} [c^\dagger(0) Q \tau_z \hat{V} \gamma_1 + \text{H.c.}]. \end{aligned} \tag{2}$$

The Kondo coupling constant $J_L = 2|t|^2/|\varepsilon|$ to the normal metal is expressed in terms of the tunneling amplitude t and the dot level position ε, with $|\varepsilon| \gg \Gamma = 2\pi|t|^2 N(0)$ [$N(0)$ is the density of states of lead electrons at the Fermi energy $\varepsilon_F = 0$]. Here $Q = \frac{1}{4} I \otimes I + [\vec{s} \cdot \vec{S}] \otimes \tau_z$ is the Nambu space extension of the exchange interaction in which $\vec{s}$ is the operator of electron spin. Within the Keldysh formalism, we use Green's functions (GF) for the normal-metal lead electrons integrated over momentum

$$\bar{g} = \frac{1}{2\pi} \Sigma_k g_k = \begin{pmatrix} \bar{g}^{11} & \bar{g}^< \\ \bar{g}^> & \bar{g}^{22} \end{pmatrix},$$

with entries as 4×4 diagonal matrices,

$$\begin{aligned} \bar{g}^{11}(\omega) &= \bar{g}^{22}(\omega) = \frac{i}{2} N(0)[I - \text{diag}(f_-, f_-, f_+, f_+)], \\ \bar{g}^<(\omega) &= -\bar{g}^>(-\omega) = iN(0)\text{diag}(f_-, f_-, f_+, f_+), \end{aligned}$$

where $f_\pm = f(\omega \pm eV)$, $f(\omega)$ being the Fermi distribution function for the metal lead electrons. The GF matrix in a rotated Keldysh basis is defined as $\tilde{g} = K \bar{g} \hat{\rho}_z K^{-1}$, where the Pauli matrices $\hat{\rho}$ act in Keldysh space and

$$K = \frac{1}{\sqrt{2}} \begin{pmatrix} 1 & -1 \\ 1 & 1 \end{pmatrix}.$$

The energy gap Δ of the superconductor is taken to be the highest energy scale. At low bias $eV < \Delta$, and in the weak coupling limit $T \gg T_K$, it is justified to project the Majorana quasiparticle operator in the superconductor on its zero energy sector [18,19]. To average over a product of dot spin operators we express them in terms of mixed Dirac $(f, f^\dagger)$ and Majorana (η_x, η_y, η_z) fermions [20]: $S_+ = \eta_z f^\dagger$, $S_- = f\eta_z$, $S_z = -i\eta_x\eta_y$, $f = (\eta_x - i\eta_y)/\sqrt{2}$. The Keldysh GFs for these fermions are

$$\begin{aligned} F_f^<(\nu) &= 2\pi i f(B)\delta(\nu - B), & F_f^R(\nu) &= \frac{1}{\nu - B + i\delta}, \\ F_z^<(\nu) &= \pi i \delta(\nu), & F_z^R(\nu) &= \frac{1}{\nu + i\delta}. \end{aligned} \tag{3}$$

The components of the Keldysh matrix GF of the Majorana fermions at the ends of TS as derived from H_M [Eq. (2)] are given by $[G^R]^{-1} = \frac{1}{2}[i\partial_t - 2i\hat{\nu}]$, $G^<(\omega) = -2if(\omega)\,\text{Im}G^R(\omega)$.

Nonlinear conductance: weak coupling regime.—The current operator is $\hat{J} = e\frac{d\hat{N}_L}{dt} = \frac{ie}{\hbar}\frac{t}{|\varepsilon|} c^\dagger(0) Q \hat{V} \gamma_1 + \text{H.c.}$, where $\hat{N}_L$ is the number operator of the normal-metal lead. Evaluating the current diagrams in the weak coupling limit (Fig. 2) yields the total conductance $\sigma = \frac{dJ}{dV}$ up to third order in J_L,

$$\sigma = \alpha W(2\nu)\left\{1 + 3\left[R(B) + \frac{\Gamma K(B)}{\pi|\varepsilon|}\right]\right\} \equiv \sigma^p + \sigma^{ex}, \tag{4}$$

where $\alpha = \frac{\pi e^2}{2h}\Gamma|\lambda|^2/(T\varepsilon^2)$ is the tunneling rate and

$$\begin{aligned} W(x) &= \left(\cosh^{-2}\frac{x + eV}{2T} + \cosh^{-2}\frac{x - eV}{2T}\right)\Big/2, \\ R(B) &= [r(B) + r(-B)]/3; \\ K(B) &= \kappa(B) + \kappa(-B), \\ r(B) &= \frac{1}{2}\cosh^{-2}\frac{B}{2T} + \frac{W(B + 2\nu)}{W(2\nu)}\left(1 + \tanh\frac{B}{2T}\tanh\frac{\nu}{T}\right), \\ \kappa(B) &= \frac{1}{6}\cosh^{-2}\frac{B}{2T} L(2\nu + B) + \frac{W(2\nu - B)}{W(2\nu)}[L(2\nu) \\ &\quad + L(2\nu - B)]\left(1 - \tanh\frac{B}{2T}\tanh\frac{\nu}{T}\right). \end{aligned}$$

There is a clear separation between potential and spin scattering. The third order contribution to the conductance includes large logarithmic terms, that is the hallmark of the Kondo effect in a tunneling system with topological superconductor. They are associated with the function $L(x) = \frac{1}{2}[\ln\frac{D}{\sqrt{(x-eV)^2+T^2}} + \ln\frac{D}{\sqrt{(x+eV)^2+T^2}}]$ (here the bandwidth D serves as a high energy cutoff). Only these dominant logarithmic terms are retained. In the zero field limit $(B \to 0)$ $R(B) \to 1$, $K(B \to 0) = L(2\nu)$, and the total conductance becomes

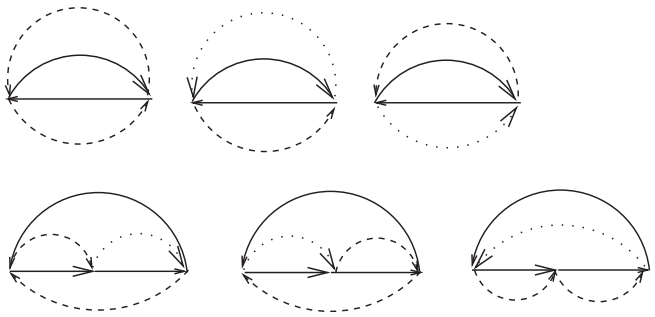

FIG. 2. Diagrams contributing to the conductance due to the Kondo interaction (2). Upper (lower) panel represents second (third) order contributions. Thick solid line: Majorana GF; thin solid lines: lead fermions GF dashed and dotted lines: impurity spin. Dotted line is the Majorana F_z GF, and dashed line is the Dirac fermion F_f GF. The left vertex in both sets has Keldysh index 1, other vertices have σ_z Pauli matrix acting in Keldysh space.

$$\sigma = \alpha W(2\nu)\left[1 + 3\left(1 + \frac{\Gamma}{\pi|\varepsilon|}L(2\nu)\right)\right]. \qquad (5)$$

In Fig. 3 the total nonlinear conductance is displayed as function of the applied voltage. Two distinct peaks are resolved as the coupling energy ν of the MF exceeds the temperature, a fact which has natural experimental implications. This is one of the central results of the present study since it combines the Kondo and Majorana fermion physics and encourages experimental activity in searching a realization of MF. The magnetic field $B = 3$ T can exceed Δ that is strong enough to form TS in the wire

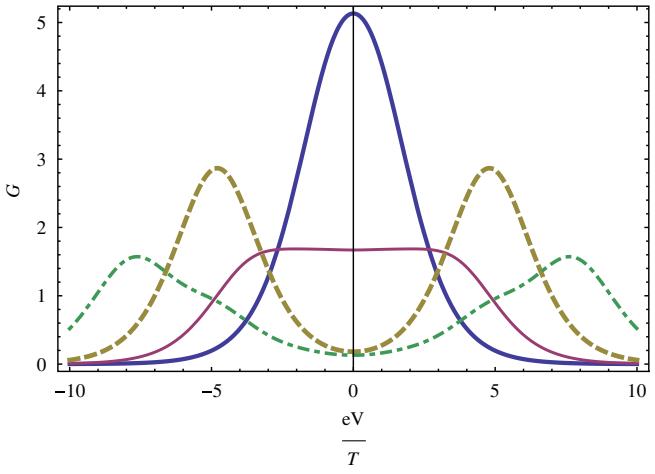

FIG. 3 (color online). The total nonlinear conductance (4) $G = \sigma/\alpha$ versus applied bias. The central high peak and lower plateau correspond to $\nu = 0.4$ T, $D = 1000$ T but different values of magnetic field: $B = 0$ for the peak and $B = 3$ T for the plateau. The same for the dashed and dotted dashed curves, the only difference is that $\nu = 2.4$ T. For all four curves we assume $\Gamma/(2\pi\varepsilon) = 0.1$.

without interaction. Under magnetic field the heights of the peaks decrease and reveal the more complicated structure of $\sigma(V)$. Kondo correlations can also be studied through the temperature dependence of the zero bias conductance G^t in the region $T_K < T < \Gamma$, as displayed in Fig. 4. Note that G^t in Fig. 4 correlates with Fig. 3: For $T_K < T < \nu$ the total zero bias conductance strongly decreases with T, while for $\nu < T$ it has a shallow peak.

The Kondo temperature $T_K = D\exp[-\pi|\varepsilon|/\Gamma]$ is determined solely by interaction with the normal-metal lead. The poor-man's scaling renormalization group (RG) equations read

$$\frac{dJ_L}{d\ln D} = -N(0)J_L^2, \qquad \frac{dJ_{LR}}{d\ln D} = -N(0)J_L J_{LR}, \qquad (6)$$

where $J_{LR} = 2t|\lambda|/|\varepsilon|$. The solution of these equations defines the above expression for the Kondo temperature and the conductance,

$$G_{\text{peak}} = \frac{\pi^2 e^2}{h}\frac{\lambda^2}{|t|^2}\frac{W(2\nu + B)}{N(0)T}\frac{1}{\ln^2(\frac{d(\nu,B)}{T_K})}, \qquad (7)$$

where $d(\nu, B) = \{(T^2 + 4\nu^2)[T^2 + (2\nu + B)^2]\}^{1/4}$. The RG equations (6) show that the Kondo instability is related to the normal-metal lead while the impact of resonance tunneling through the MBS on T_K is irrelevant. The scaling invariance of the exchange part of the conductance implies $d\sigma^{ex}/d\ln D = 0$, in agreement with the second RG equation (6).

Zero bias conductance: strong coupling regime $T < T_K$.—Here, the mean field slave boson approximation (MFSBA) is used to evaluate the zero bias tunneling conductance. As in the weak coupling limit, we neglect the

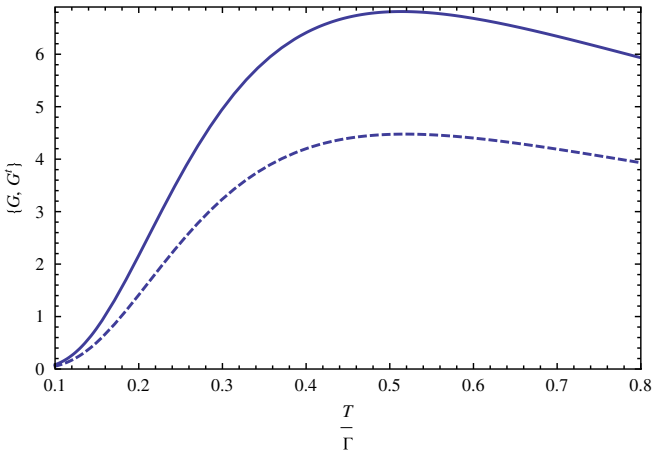

FIG. 4 (color online). Zero bias conductance as function of temperature in the region $T_K < T < \Gamma$ at zero magnetic field. $G = \sigma^{(2)}/(\alpha T/\Gamma)$ is the second order contribution (dashed line), while G^t stands for the total conductance in the same units as G (solid line). We take $\nu = 0.4\Gamma$ and use the value $\Gamma/(2\pi\varepsilon) = 0.1$.

continuous spectrum above the superconductor gap (in the weak coupling limit this condition is automatically satisfied and the MBS effectively represent the topological superconductor). To implement it in the strong coupling limit we assume the inequality $\Gamma_S < \Gamma$ (in addition to the conditions $\Delta \gg T,\ eV, T_K$). Here Γ_S is the tunneling width into the TS. Then the contribution to the conductance from the continuous spectrum, proportional (at resonance) to $\sigma_c \sim 4(\Gamma_S/\Gamma)^2$, is indeed very small [21]. Thus, if $T \leq T_K$, then, unlike the case $T \gg T_K$, the condition $\Delta \gg T_K$ has to be supplemented by the inequality $\Gamma_S < \Gamma$ in order to justify the small contribution of the continuous spectrum of the superconductor. If the magnetic field is excluded from the dot it may be strong, $B > \Delta$. Otherwise, $B < T_K$ to ensure the Kondo effect. This is below the window for achieving the TS phase in the noninteraction limit. However, the strong interactions prevailing in the dot can favor the TS phase even for weak magnetic fields [16(b)].

In the limit $U \to \infty$ (1), employing the slave boson technique, the dot is empty or singly occupied. The electron creation operator is written as $d_\sigma^\dagger = f_\sigma^\dagger b$, where the slave fermion $f_\sigma^\dagger$ and the slave boson b mimic the singly occupied and empty dot states. The constraint $\sum_\sigma d_\sigma^\dagger d_\sigma + b^\dagger b = 1$ is encoded by including a Lagrange multiplier η_c in the total action S. At the mean field level the constraint is satisfied only on the average.

The partition functional $Z(\theta_q)$ is computed by integrating the action over slave fermion and Majorana fields. Here the source field θ_q is coupled to the current operator $\hat{I} = iet d^\dagger c(0)/\hbar + \text{H.c.}$. The resulting effective action (in the MFSBA) is Gaussian and depends on two c-number parameters: the boson field b_0 and the chemical potential (Lagrange multiplier) η_c. Integrating the effective action leads to the fermion part of the partition function,

$$\ln Z_f(\theta_q) = \text{tr}\ln\left\{\frac{-i}{2}(G_f^{-1} - \theta_q \Gamma b_0^2 \tau_z[\tilde{g}, \hat{\rho}_x])\right\}, \qquad (8)$$

where $G_f^{-1} = G_{f0}^{-1} - b_0^2\hat{\Gamma}$ is the inverse dot total GF and trace is carried out over Keldysh space as well. The inverse GF $[G_{f0}^{-1R}] = \sigma_0 \otimes (i\partial_t - \tilde{\varepsilon}\tau_z)$ describes the noninteracting level with energy shift $\varepsilon \to \tilde{\varepsilon} = \varepsilon + \eta_c$. The vertex matrix reads $\hat{\Gamma} = \Gamma\tilde{g} + \tau_z \hat{V} G_{11} \hat{\rho}_x \hat{V}^\dagger \tau_z$. Here,

$$G_{11} = \begin{pmatrix} G_{11}^K & G_{11}^R \\ G_{11}^A & 0 \end{pmatrix}$$

is the Majorana GF of the γ_1 state. The matrix elements of $\hat{\Gamma}$ are obtained,

$$\begin{aligned} 2\,\text{Im}\Gamma^R(\omega) &= -\Gamma + 2|\lambda|^2\,\text{Im}G_{11}^R(\omega)(1 - \hat{\Omega}), \\ \Gamma^K(\omega) &= \Gamma\tilde{g}^K + 2i|\lambda|^2(1 - \hat{\Omega})\tanh\frac{\omega}{2T}\,\text{Im}G_{11}^R, \end{aligned} \qquad (9)$$

where $\hat{\Omega} = \sigma_y \otimes \tau_z + \sigma_z \otimes \tau_x + \sigma_x \otimes \tau_y$. The current is given by

$$I = \frac{\partial \ln Z}{\partial \theta_q} = \frac{-ie\Gamma b_0^4}{2\hbar}\,\text{tr}[(G_f^R\Gamma^K G_f^A + 2G_f^R\,\text{Im}\Gamma^R G_f^A \tilde{g}^K)\tau_z]. \qquad (10)$$

The MFSBA is quite reliable in equilibrium $V \to 0$. Therefore, we consider below the temperature dependence of the zero bias conductance for different couplings between two MBS. In equilibrium, the mean field solutions for b_0 and η_c minimize the free energy F, yielding $F = -T\sum_{\omega_n}\text{tr}\ln[G_f^{-1}(\omega_n)] + \eta_c b_0^2$, where the last term is the slave boson part of the free energy due to the constraint. The Matsubara GF of the dot, G_f, is easily obtained from $G_f^R(\omega)$. Because of the conditions $\Gamma_S < \Gamma$ and $T_K \ll \Delta$, the contribution of the continuous spectrum above the superconducting energy gap can be neglected. The mean field equations are

$$\begin{aligned} b_0^2 - 1 &= -T\sum_{\omega_n}\text{tr}[\tau_z G_f(\omega_n)], \\ \eta_c &= -T\sum_{\omega_n}\text{tr}[G_f(\omega_n)\hat{\Gamma}(\omega_n)], \end{aligned}$$

where the first equation fixes the level position $\tilde{\varepsilon}$. In the Kondo regime the level is singly occupied, $\tilde{\varepsilon} = 0$ for $\eta_c = |\varepsilon|$. This approximate solution of the second equation for η_c is inserted in the first equation to yield a nontrivial solution ($b_0 \neq 0$) for the boson field in terms of the Kondo temperature. Nonlogarithmic terms in the second equation are discarded in the Kondo regime. Direct calculations show that such logarithms appear only for normal-metal lead and all terms related to the MBS can be safely neglected. Thus, $b_0^2\Gamma/2 = T_K$ (T_K was defined above for the N lead), in agreement with the weak coupling analysis (6). For $T < T_K$, Eq. (10) yields a close expression for the linear conductance

$$\frac{\sigma}{G_0} = g_\Gamma^2 g_\lambda^2 \int_0^\infty \frac{dx}{\cosh^2 x}\,\frac{u^2(x) + v^2(x)}{(x^2 + g_\Gamma^2)A(x)}, \qquad (11)$$

where $A(x) = x^2 + [g_\Gamma - g_\lambda v(x)]^2 + g_\lambda^2 u^2(x) - 2x g_\lambda v(x)$, $G_0 = 2e^2/h$, and the real functions u, v are defined from $u(x) + iv(x) = x/[(x + i\delta)^2 - \tilde{\nu}^2]$. Pertinent dimensionless parameters are the interaction energy of MF $\tilde{\nu} = \nu/T$ and the tunneling rates $g_\Gamma = \Gamma b_0^2/4T = T_K/2T$, $g_\lambda = 2|\lambda|^2 b_0^2/T^2$. Figure 5 displays the linear conductance at zero bias versus temperature for two values of the Majorana fermion coupling energy ν and $|\lambda|^2 = \Gamma T_K/8$. It displays a similar dependence on temperature as in the weak coupling limit $T > T_K$ shown in Fig. 4. In both cases, when $\nu < T$, the fall off of the peak occurs at lower temperature, whereas for $\nu > T$ a wide and shallow dip emerges.

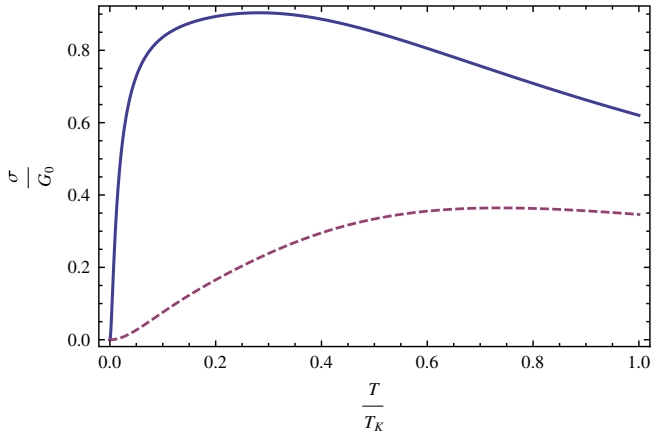

FIG. 5 (color online). The zero biased conductance as a function of temperature at zero magnetic field in the strong coupling limit ($T < T_K$). The dashed curve corresponds to $\nu = 0.5T_K$ and the solid line to $\nu = 0.1T_K$.

Conclusions—The Keldysh technique has been employed to calculate the linear and nonlinear conductance in a system consisting of a quantum dot (tuned to the Kondo regime) connected to a metal lead on the left side and 1D TS hosting Majorana bound states on the right side. Under certain approximations the problem reduces to that of a NM-QD-MBS tunneling system in both the weak ($T \gg T_K$) and strong ($T < T_K$) coupling limits. Renormalization group analysis is performed in the weak coupling limit while the MFSBA is used at $T < T_K$. When the coupling energy ν of MBS exceeds the temperature, the conductance has a two peak structure. Under a constant magnetic field, Zeeman splitting occurs on the dot and reduces the heights of the peaks. The magnetic field may result in a more complicated peak structure of the nonlinear conductance. Our analysis shows that in an attempt to probe the features of Majorana fermion physics, the role of the Kondo effect is decisive. It is manifested by the occurrence of a strong temperature dependence of the zero bias conductance and exposes distinct behavior of the nonlinear conductance as compared with that of the simpler NM-MBS tunnel junction.

We would like to thank A. Rosch and D. Loss for stimulating discussions. This research was supported by The Israeli Science Foundation grants [No. 1078/07, (A. G.) and No. 1703/08 (Y. A.)].

[1] L. Fu and C. L. Kane, Phys. Rev. Lett. **100**, 096407 (2008).
[2] M. Sato and S. Fujimoto, Phys. Rev. B **79**, 094504 (2009).
[3] Y. Oreg, G. Refael, and F. von Oppen, Phys. Rev. Lett. **105**, 177002 (2010).
[4] J. Alicea, Phys. Rev. B **81**, 125318 (2010).
[5] R. M. Lutchyn, J. D. Sau, and S. Das Sarma, Phys. Rev. Lett. **105**, 077001 (2010).
[6] A. C. Potter and P. A. Lee, Phys. Rev. Lett. **105**, 227003 (2010).
[7] X.-L. Qi and S.-C. Zhang, arXiv:1008.2026 [Rev. Mod. Phys. (to be published)].
[8] J. Nilsson, A. R. Akhmerov, and C. W. J. Beenakker, Phys. Rev. Lett. **101**, 120403 (2008).
[9] C. Nayak, S. Simon, A. Stern, M. Freedman, and S. Das Sarma, Rev. Mod. Phys. **80**, 1083 (2008).
[10] A. Y. Kitaev, Phys. Usp. **44**, 131 (2001).
[11] L. Fu and C. L. Kane, Phys. Rev. B **79**, 161408 (2009).
[12] C. J. Bolech and E. Demler, Phys. Rev. Lett. **98**, 237002 (2007).
[13] K. T. Law, P. A. Lee, and T. K. Ng, Phys. Rev. Lett. **103**, 237001 (2009).
[14] J. Linder, Y. Tanaka, T. Yokoyama, A. Sudbø, and N. Nagaosa, Phys. Rev. Lett. **104**, 067001 (2010).
[15] K. Flensberg, Phys. Rev. B **82**, 180516(R) (2010).
[16] (a) J. Alicea, Y. Oreg, G. Refael, F. von Oppen, M. P. A. Fisher, arXiv:1006.43950; (b) E. M. Stoudenmire, J. Alicea, O. A. Starykh, and M. P. A. Fisher, Phys. Rev. B **84**, 014503 (2011).
[17] J. D. Sau, S. Tewari, and S. Das Sarma, Phys. Rev. A **82**, 052322 (2010).
[18] M. Leijnse and K. Flensberg, arXiv:1012.4650.
[19] L. Fu, Phys. Rev. Lett. **104**, 056402 (2010).
[20] O. Parcollet and C. Hooley, Phys. Rev. B **66**, 085315 (2002).
[21] P. Schwab and R. Raimondi, Phys. Rev. B **59**, 1637 (1999).